ABCM Symposium Series in Mechatronics

Regularizations for a Black Box EIT algorithm

Julio C. C. Aya
Department of Mechanical Engineering - Polytechnic School of University of São Paulo Av. Prof. Mello de Moraes, 2231 - São Paulo - SP - 05508-900, Brazil
jccaya@usp.br

Fernando Silva de Moura
Department of Mechanical Engineering - Polytechnic School of University of São Paulo Av. Prof. Mello de Moraes, 2231 - São Paulo - SP - 05508-900, Brazil
fernando.moura@poli.usp.br

Pai Chi Nan
Department of Mechatronic and Mechanical Systems Engineering - Polytechnic School of University of São Paulo Av. Prof. Mello de Moraes, 2231 - São Paulo - SP - 05508-900, Brazil
pai.nan@poli.usp.br

Ronaldo K. Schweder
Department of Mechanical Engineering - Polytechnic School of University of São Paulo Av. Prof. Mello de Moraes, 2231 - São Paulo - SP - 05508-900, Brazil
ronaldo.schweder@poli.usp.br

Raul Gonzalez Lima
Department of Mechanical Engineering - Polytechnic School of University of São Paulo Av. Prof. Mello de Moraes, 2231 - São Paulo - SP - 05508-900, Brazil
rauglima@usp.br

Abstract.
One of the objectives of Electrical Impedance Tomography (EIT) is to estimate the resistivity distribution based on measurements of electric potential on the boundaries of a domain of interest. In this work we propose an algorithm that identifies directly the back-projection matrix given known perturbations of the resistivity distribution and their associated boundary electric potential perturbations, called Black Box algorithm, two new regularizations for the Black Box algorithm. One of the new regularizations have his performance compared to two classical regularization methods: truncation of singular values and Tikhonov regularization.
Keywords: *black-box, Electrical Impedance Tomography, inverse problem*

1. Introduction

The Electrical Impedance Tomography (EIT) is a method to estimate the impedance distribution in a domain. This domain can be discretized through the Finite Elements Method (FEM) and the variable of interest, the impedance distribution or variations in time of the impedance distribution, turn out to be the vector of impedance of each finite element. The problem of estimating the impedance distribution knowing the injected current, measuring electric potentials on the boundary of the domain and knowing the structure of the model can be classified as an inverse problem.

The impedance value of different biological tissues is governed fundamentally by the concentration of different fluids (blood, water, air). This is the reason why EIT has being applied to monitor gastric functions, the oesophagus, lung ventilation, pulmonary edemas and brain clots, for instance. It is possible to say that the lung is a privileged tissue for being monitored by EIT because its impedance is a function of the air content and blood content, which suffer changes during the respiratory and cardiac cycles.

Initial work by Brown (Barber and Brown, 1984) used an isopotential approach for solving the inverse problem. The backprojection method is based on linearization and delivers difference images. This algorithm can be described as follows: Two different sets of measurements are required, the first set of voltages V_0 is a reference set of measurements. The second set of measurements V_1 is related to the modified impedance distribution. An estimate of the normalized resistivity change can be computed from the formula

$$\Delta\rho = \mathbf{B}\Delta V \tag{1}$$

where

$$\Delta\rho = \frac{\rho_1 - \rho_0}{\rho_0}$$
$$\Delta V = \frac{V_1 - V_0}{V_0},$$

and $\mathbf{B}$ is the inverse of the sensitivity matrix, the construction of which can be found in (Santosa and Vogelius, 1990 and Guardo *et.al.*, 1991).

The objective of this work is to obtain an algorithm to identify directly the $\mathbf{B}$ matrix, using a set of chosen difference images, and a set of accurately computed boundary data, obtained through a FEM model. The determination of $\mathbf{B}$ through the algorithm proposed involves inversion of an ill-conditioned matrix. Four procedures are used, two classical regularization methods:

1. Truncation of singular values decomposition
2. Tikhonov regularization

and two new regularizations methods:

3. Heuristic
4. Filtered columns of B

2. Theory

Consider a closed domain with unknown electromagnetic properties. The objective of the EIT is to estimate the impedance distribution of the domain, given the excitation current imposed at the boundary and the electric potentials measured in some regions of the boundary. The current is imposed accurately. And the electric potentials are measured by a finite number of attached electrodes. Therefore, the information about the domain is limited.

There are several ways to inject current into the domain. An injection pattern must be chosen, for instance, inject current into one electrode and removing from another electrode, skipping one electrode (fig. 1). Each *current pattern* is defined by a pair of injection electrodes.

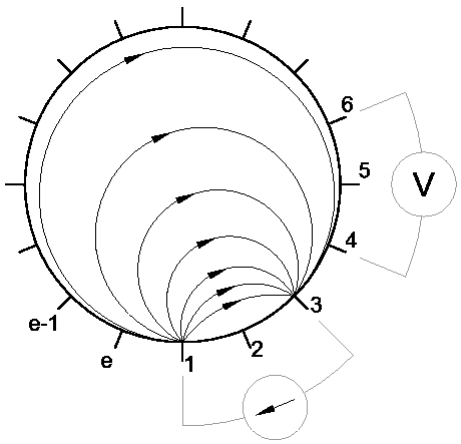

Figure 1. Current pattern and voltage measurement.

For each current pattern, the electric potential between pairs of electrodes are measured. After gathering the potential data from the current patterns it is possible estimate the resistivity distribution of the domain by solving the following set of equations (Trigo, Gonzalez-Lima and Amato, 2004):

$$\nabla \cdot \left(\frac{1}{\rho}\nabla\Psi\right) = 0 \tag{2}$$
$$\int_{\partial\mathbf{\Gamma}_j} \frac{1}{\rho}\frac{\partial\Psi}{\partial\vec{\hat{n}}} = c_j \tag{3}$$
$$\frac{1}{\rho}\frac{\partial\Psi}{\partial\vec{\hat{n}}} = 0 \tag{4}$$
$$\Psi + z_j\frac{1}{\rho}\frac{\partial\Psi}{\partial\vec{\hat{n}}} = v_j \tag{5}$$

The eq. (2) represents the electric potential (Ψ) inside the domain and ρ is the resistivity. The eq. (3) represents the current (c_j) crossing the j-þth electrode on the boundary. Eq. 4 represents the null current crossing the boundary not attached to electrodes. Finally, eq. (5) represents the skin-electrode interface impedance, on the j-*th* electrode (z_j), influence on the measured potential v_j.

It is common to define two problems in EIT. In the, so called, *Forward Problem* the resistivity distribution, the current patterns, the structure of the model are known and the electrode electric potentials are desired. In the, so called, *Inverse Problem*, the electrode potentials, the current patterns are known and the resistivity distribution of the domain is desired.

2.1 Forward Problem

The forward problem in EIT computes the potentials in the electrodes. The electric model, using the FEM of a domain, leads to the following equation (Logan, 1986) and (Sadiku, 1992):

$$Y(\rho) \cdot V = C, \tag{6}$$

where $Y(\rho)$ is the conductivity matrix, $V = [v_1, \ldots, v_e]$ is a matrix of potentials, each column of this matrix is composed by nodal electric potentials associated to each current pattern, $C = [c_1, \ldots, c_e]$ is a matrix of current patterns each column represents a current pattern. Both c_j and v_j are vectors with e elements, where q denotes a node of the mesh.

In order to solve eq.6 it is necessary to remove the singularity of matrix $Y(\rho)$. This is done imposing the potential of a node, for example, with null value (Yorkey et. al, 1987).

2.2 Inverse Problem

The inverse problem consists on estimating the resistivity distribution inside the domain, from a set of current patterns, measurements of electric potentials in the electrodes and the structure of the model.

In the eq. (6), the conductivity matrix $Y(\rho)$ has known structure, however the parameters of resistivity are not known. Denoting the vector of electric resistivity $\rho \in \Re^n$, where n it is the number of elements of the mesh, the equation eq. (6) can be rewritten

$$V(\rho) = [Y(\rho)]^{-1} \cdot C. \tag{7}$$

It is possible to define a nonlinear map $\vec{f} : \rho \rightarrow v_j$ where v_j is a vector of electrodes potentials related to the j-th current pattern. Therefore, the vector of electric potentials at the electrodes is a nonlinear function of the distribution of resistivity. Using a truncated Taylor expansion of the $\vec{f}$ map around a reference resistivity ρ^0, leads to eq. (1).

3. Black-Box

The main idea of the black-box method is that if good images (relative variations of resistivity) and good measurements (relative variations of electrode potentials) are available, then a matrix that relate measurements and images may be estimated. The method forms a set of difference images and computes the respective variations on electrode potentials. From this two sets of information it estimates the black-box matrix $\mathbf{B}$.

The black-box algorithm estimates directly $\mathbf{B}$ matrix, given the variation of electric potentials on the boundary of the domain when the resistivity of each finite element of domain is changed, one by one. The method assumes linearity between variation of electric potentials at the electrodes and variation of resistivity.

First, it is assumed an initial resistivity distribution which will be used as reference. With this reference, the electric potentials are calculated, using a FEM, for each current injection pattern. A perturbation is imposed on each finite element, one at a time. The electric potentials at the electrodes are computed and normalized with respect to the electric potential corresponding to the reference resistivity value. A matrix of perturbed electric potentials is formed such that each column of this matrix is a perturbed electric potential vector. Through the perturbed electric potential matrix and a matrix of resistivity perturbation, the matrix $\mathbf{B}$ can be determined.

In summary, the procedure to determine $\mathbf{B}$ is:

1. assume a known resistivity at each one of n elements of domain, arrange as vector ρ^0. The linearization of the model is performed around ρ^0.
2. each current injection pattern is denoted by $\{c_j\}_{q\times 1}$ for $j = 1, 2, \ldots, e$;
3. the electric potentials at the electrodes, v_j^0, are determined from the direct problem, collecting only the electric potentials at the nodes that represent electrodes,

$$\mathbf{Y}|_{\rho^0} v_j^0 = c_j \qquad , \qquad j = 1, 2, \ldots, e. \tag{8}$$

4. a known perturbation on the resistivity of the i-*th* element of ρ^0, is denoted by $\delta\rho_i$ and $i = 1, 2, \ldots, n$;
5. vectors $\{\delta\rho^i\}_{n\times 1}$ are formed such that all elements are null but the i-*th* element that contains $\delta\rho_i$, i. e., $\delta{\rho^i}_i = \delta\rho_i$;
6. for each current pattern c_j, the electric potentials at electrodes, v_j^i related to a resistivity perturbation $\delta\rho^i$ are determined by the direct problem, collecting only the electric potentials at the nodes that represent electrodes,

$$\mathbf{Y}|_{(\rho^0+\delta\rho^i)}v_j^i = c_j \qquad , \qquad j = 1, 2, \ldots, e \qquad , \qquad i = 1, 2, \ldots, n. \tag{9}$$

7. let $\{v^0\}_{e^2\times 1}$ be an augmented vector formed of all v_j^0, such that,

$$v^0 = \begin{bmatrix} v_1^0 \\ v_2^0 \\ \cdots \\ v_e^0 \end{bmatrix} \tag{10}$$

8. let $\{v^i\}_{e^2\times 1}$ be an augmented vector formed of all v_j^i, such that

$$v^i = \begin{bmatrix} v_1^i \\ v_2^i \\ \cdots \\ v_e^i \end{bmatrix} \tag{11}$$

9. form a normalized vector $\{\psi^i\}_{n\times 1}$ such that each j element is

$$\psi_j^i = \frac{\delta{\rho^i}_j}{\rho_j^0} \tag{12}$$

10. form a normalized vector $\{\theta^i\}_{e^2\times 1}$ such that each element, is

$$\theta^i = \frac{v^i - {v^0}_j}{{v^0}_j}, \tag{13}$$

11. define a matrix $\mathbf{\Psi}_{n\times n}$ such that

$$\mathbf{\Psi} = \begin{bmatrix} \psi^1 & \ldots & \psi^i & \ldots & \psi^n \end{bmatrix}, \tag{14}$$

observe that this matrix is diagonal;

12. define a matrix $\mathbf{\Theta}_{e^2\times n}$ such that

$$\mathbf{\Theta} = \begin{bmatrix} \theta^1 & \ldots & \theta^i & \ldots & \theta^n \end{bmatrix} \tag{15}$$

13. since each column of Ψ is an image and can be related to a column of Θ by a $\mathbf{B}$ matrix, one can say,

$$\mathbf{\Psi}_{n\times n} = \mathbf{B}_{n\times e^2}\mathbf{\Theta}_{e^2\times n} \tag{16}$$

14. finally, determine the matrix $\mathbf{B}$ that minimizes an error index. Error indexes are addressed on section 4.3 and section 4.4

Once the matrix $\mathbf{B}$ is obtained, estimation of a difference image is performed multiplying $\mathbf{B}$ and a normalized vector of variation of electrode potentials related to each current injection pattern, according to eq. (17)

$$\Delta\rho = \mathbf{B}\Delta V \tag{17}$$

where $\{\Delta\rho\}_{n\times 1}$ is such that the j-*th* element is $\frac{\rho-{\rho^0}_j}{{\rho^0}_j}$ for $j = 1, 2, \ldots, n$, and $\{\Delta V\}_{e^2\times 1}$ is such that the j-*th* element is $\frac{V_{measured_j} - V^0_{measured_j}}{V^0_{measured_j}}$ for $j = 1, 2, \ldots, e^2$.

4. Determination of B

This paper describes four procedures to obtain the black-box matrix $\mathbf{B}$. This matrix is not square and the problem is ill-conditioned.

Four methods were developed for estimation of $\mathbf{B}$:

1. the first method consist on using *pseudo-inverse* calculation. This calculation is done using singular value decomposition (SVD) and singular value truncation.
2. the second method uses a Tikhonov regularization, which is determination of a smoother approximated solution compatible with the data observed for a certain level of noise, introducing a priori information, that changes the matrix to well-posed.
3. the third method will be denominated *Heuristic regularization*
4. the four method will be called *Filtered B regularization*

4.1 Truncating the Singular Values

Any matrix can be decomposed into three matrices U, S and V (Watkins 1991),

$$\mathbf{\Theta} = USV^T \tag{18}$$

where

$\Rightarrow$ $U \in \Re^{e^2 \times n}$ is an orthonormal matrix

$\Rightarrow$ $S \in \Re^{n \times n}$ is a diagonal matrix containing singular values of $\mathbf{\Theta}$

$\Rightarrow$ $V \in \Re^{n \times n}$ is an orthonormal matrix

with the matrix decomposed, its pseudo-inverse is computed as

$$\mathbf{\Theta}^{+} = VS^{-1}U^T, \tag{19}$$

where S^{-1} is computed as

$$S^{-1}(i,i) = \begin{cases} \frac{1}{S(i,i)} & \text{if } S(i,i) > \xi \\ 0 & \text{if } S(i,i) \leq \xi \end{cases} \tag{20}$$

and ξ is the parameter to determine which singular values will be used.

Now, the matrix $\mathbf{B}$ is determined as

$$\mathbf{B} = \mathbf{\Psi}\mathbf{\Theta}^{+} \tag{21}$$

4.2 Tikhonov Regularization

To solve an ill-conditioned problem it is necessary additional information. Tikhonov and Arsenin (1977) proposed a general formulation, called regularization or method of regularization. The inverse problem is formulated as an optimization problem.

The error can be defined as

$$\mathbf{E} = \mathbf{\Psi}^T - \mathbf{\Theta}^T\mathbf{B}^T \tag{22}$$

and the error index is defined as

$$IE = \mathbf{E}^T\mathbf{E} + \lambda\mathbf{B}\mathbf{B}^T, \tag{23}$$

and, when minimized in respect to $\mathbf{B}$, leads to

$$\mathbf{B} = \mathbf{\Psi}^T\mathbf{\Theta}^T\left[\mathbf{\Theta}\mathbf{\Theta}^T + \lambda\mathbf{I}\right]^{-1} \tag{24}$$

where $\mathbf{I} \in \Re^{e^2 \times e^2}$ is the identity matrix and λ is a scalar parameter.

4.3 Heuristic Regularization

The matrix $\mathbf{\Theta}^T\mathbf{\Theta}$ is ill-conditioned. The inversion of $\mathbf{\Theta}^T\mathbf{\Theta}$ for $\mathbf{B}$ determination introduce great numerical errors. Therefore, to determine $\mathbf{B}$, a regularization is necessary.

An error index is defined as,

$$IE = tr\left\{\mathbf{E}^T\mathbf{E} + \alpha\mathbf{B}^T\mathbf{F}^T\mathbf{F}\mathbf{B} + \beta\mathbf{B}^T\mathbf{M}^T\mathbf{M}\mathbf{B}\right\}, \tag{25}$$

where $\mathbf{F}$ is a high pass spatial filter considering each column of $\mathbf{B}$ like an image, $\mathbf{M}$ is a matrix for improving the uniformity of the sensitivity, α and β are regularization parameters, and matrix $\mathbf{E}$ is defined as

$$\mathbf{E} = \mathbf{\Theta}(\mathbf{\Psi} - \mathbf{B}\mathbf{\Theta}). \tag{26}$$

The matrix $\mathbf{M}$ is a diagonal matrix such that each element of the diagonal is

$$m_{i,i} = r(i)^p, \tag{27}$$

where $r(i)$ is the distance of the geometrical center of the i-*th* finite element to the center of the domain, divided by the radius of the domain. And p is an experimentally adjusted real parameter, to penalize the non-uniform sensitivity.

The minimum of the error index with respect to $\mathbf{B}$ is achieved when,

$$\mathbf{B} = (\mathbf{\Theta}^T\mathbf{\Theta} + \alpha\mathbf{F}^T\mathbf{F} + \beta\mathbf{M}^T\mathbf{M})^{-1}\mathbf{\Psi}\mathbf{\Theta}^T. \tag{28}$$

4.4 Filtered columns of B

The error index is defined at the eq. (25), but the matrix $\mathbf{E}$ is redefined as

$$\mathbf{E} = (\mathbf{\Psi} - \mathbf{B}\mathbf{\Theta}). \tag{29}$$

The minimum of the error index with respect to $\mathbf{B}$ is achieved when,

$$\mathbf{B}\mathbf{\Theta}\mathbf{\Theta}^T + (\alpha\mathbf{F}^T\mathbf{F} + \beta\mathbf{M}^T\mathbf{M})\mathbf{B} = \mathbf{\Psi}\mathbf{\Theta}^T. \tag{30}$$

Note that the equation above is like the Sylvester equation:

$$AXB^T + CXD^T = E, \tag{31}$$

where A and C has the sizes $n \times n$, B and D are $e^2 \times e^2$, and E is $n \times e^2$.

Algorithms to solve Sylvester's equation were published by (Bartels *et.al* (1972)) and (Gardiner *et.al* (1992)). To determine $\mathbf{B}$, $A = \alpha\mathbf{F}^T\mathbf{F} + \beta\mathbf{M}^T\mathbf{M}$, $B = I$, $C = I$, $D = \mathbf{\Theta}\mathbf{\Theta}^T$ e $E = \mathbf{\Psi}\mathbf{\Theta}^T$.

5. Parameters and methodology

The mesh used to create the matrix $\mathbf{B}$ has 300.0 mm of diameter, $n = 2034$ pentahedrical elements (prisms of triangular base), divided equally in three layers, 30.0 mm of total height and $e = 30$ electrodes. The Figure 2 shows the top view of the mesh.

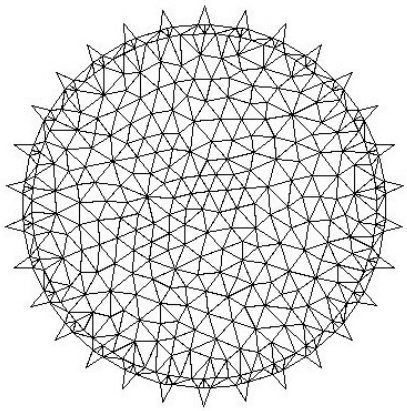

Figure 2. Finite Element Mesh.

Figure 3. Experimental Container.

The initial distribution of resistivity ρ_0 was homogeneous and equal to $3.0\,\Omega m$. The electrodes parameters were all equal to $0.02\,\Omega m^2$. The imposed perturbation $\delta\rho_i$ was $+30\%$ of initial value ρ_0.

The electric potential data set was collected from an experimental cylindrical container shown on Fig. 3 filled with 4.5% saline solution. An acrylic cylinder with 32 mm of diameter was used to simulate a region with different resistivity. The object will be analyzed on two positions. Position 1 has the object placed at the center of the container. Position 2 has the object placed 120 mm apart from the center.

6. Results

Eight images resulting from experimental data are presented. The first two images were obtained through the back-projection algorithm as described by Santosa and Vogelius (1990).

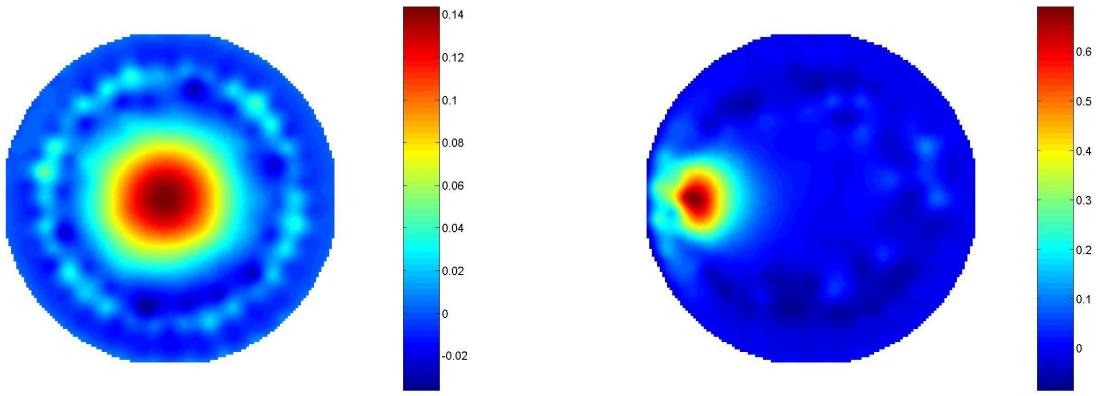

(a) Object in position 1 (b) Object in position 2

Figure 4. Images using Santosa and Vogelius algorithm.

6.1 Truncation of Singular Values

The following images were obtained from experimental data using truncation of singular values. The image at Fig. 5(a) represent the object placed at position 1 with $\xi = 0.01$ which represent the use of only 8% of all the singular values and the image at Fig. 5(b) represent the object placed at position 2 with $\xi = 0.0006$ witch represent the use of only 15% of all singular values.

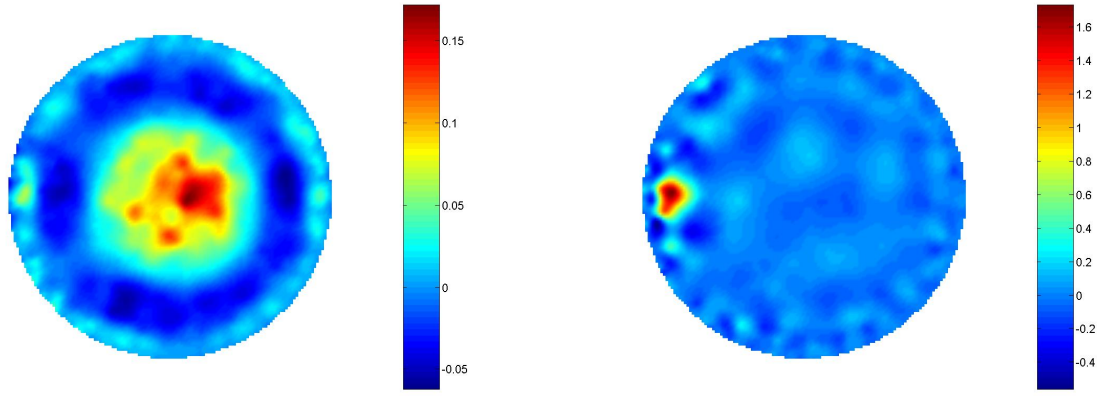

(a) Object in position 1 (b) Object in position 2

Figure 5. Images using truncation of singular values.

6.2 Tikhonov Regularization

The following images were obtained from experimental data using Tikhonov regularization. The image at Fig. 6(a) represent the object when placed at position 1 with $\lambda = 1.0\,\text{e-}5$ and the image at Fig. 6(b) represent the object when placed at position 2 with $\lambda = 1.0\,\text{e-}4$.

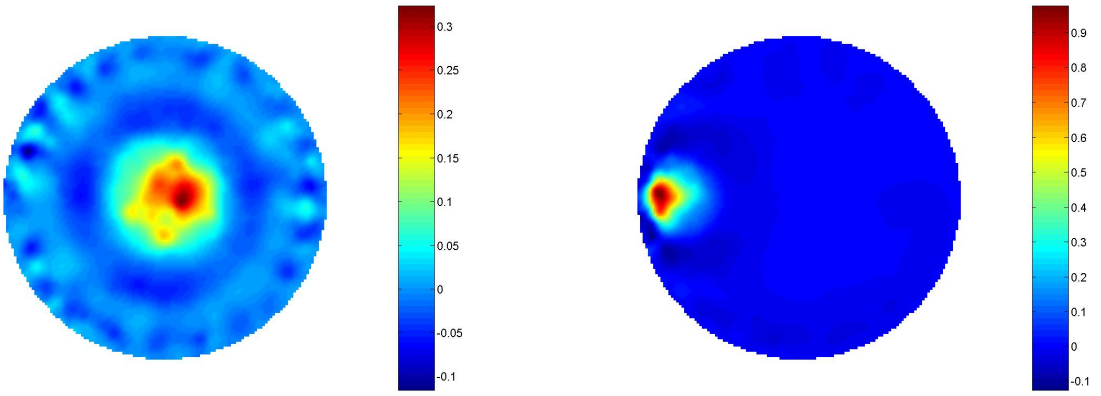

(a) Object in position 1 (b) Object in position 2

Figure 6. Images using Tikhonov Regularization

6.3 Heuristic Regularization

The following images were obtained from experimental data using heuristic regularization. For this regularization, $\alpha = 1.0\,\text{e-}4$ and $\beta = 4.0\,\text{e-}3$ were chosen. The image at Fig. 7(a) represent the object when placed at position 1 and the image at Fig. 7(b) represent the object when placed at position 2.

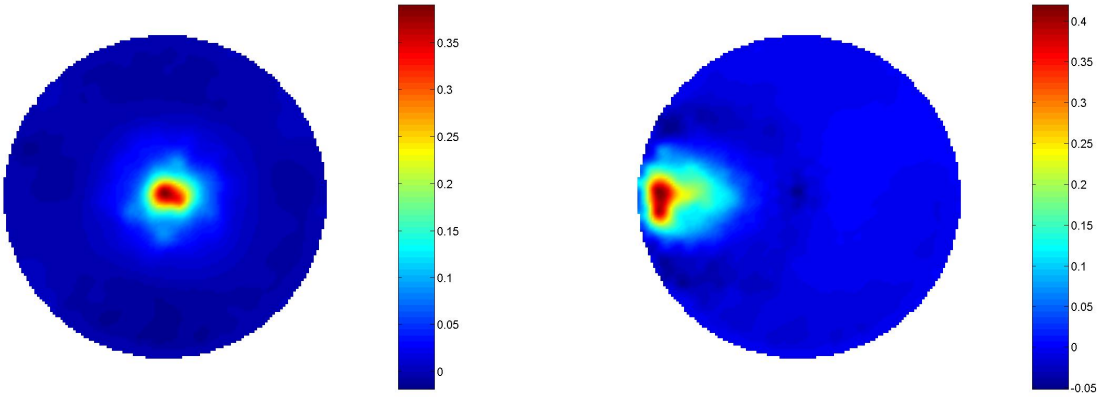

(a) Object in position 1 (b) Object in position 2

Figure 7. Images using Heuristic Regularization

7. Conclusion

It can be seen that the images obtained by these algorithms are compatible with the correct positions of the objects, and the best resolution is obtained using the Heuristic regularization. The numerical solution of the *Filtered B* regularization is under development. Our results, so far, are not appealling.

The regularization for improving the uniformity of the sensitivity proved to be efficient. The maximum values of pixels for images when the object is at the boundary or at the center using heuristic algorithm, are similar due to a proper choice of parameter β, which reduces the non-uniformity of the sensitivity.

8. Acknowledgments

Financial support by The State of São Paulo Research Foundation, process 01/05303-4 are gratefully acknowledged.

9. References

Adler, A.,1995, "Measurement of Pulmonary Function with Electrical Impedance Tomography", Ph.D., Université de Montréal.

Barber, D.C. and Brown, B.H.,1984, "Applied Potential Tomography", Journal of Physics E: Scientific Instruments, vol. 17, No. 9, pp.723 - 733.

Bartels R.H. and Stewart G.W., 1972, "Solution of the Matrix Equation $AX + XB = C$" Communications of ACM, Vol. 15, No. 9, pp. 820-826.

Brown, B.H.,2003, "Electrical impedance tomography (EIT): A review", Journal of Medical Engineering and Technology, vol. 27, No. 3, pp.97 - 108.

Gardiner J.D., Laub, A.J., Amato, J.J. and Moler C.B., 1992, " Solution of the Sylvester Matrix Equation $AXB^T + CXD^T = E$", ACM Transactions on Mathematical Software, Vol 18, No 2, pp. 223-231.

Hua, P., Woo, E.J., Webster, J.G. and Tompkins, W.J.,1993, "Finite element modeling of electrode-skin contact impedance in electrical impedance tomography", IEEE Transactions on Biomedical Engineering, vol.40, No. 4, pp.335 - 343.

Logan, D., 1986, A First Course in the Finite Element Methods, Boston : PWS Engineering.

Sadiku, N., 1992, Numerical Techniques in Electromagnetics, Boca Raton : Crc Press.

Santosa, F. and Vogelius, M.,1990, "Backprojection algorithm for electrical impedance imaging", SIAM Journal on Applied Mathematics, vol.50, No. 1, pp.216 - 243.

Tikhonov, A. and Arsenin, V., 1977, *Solution of Ill-posed Problems*. New York : John Wiley & Sons.

Trigo, F. C., Gonzalez-Lima R., Amato M. B. P., 2004, "Electrical Impedance Tomography Using the Extended Kalman Filter", IEEE Transactions on Biomedical Engineering, vol.51, No. 1, pp.72 - 81.

Yorkey, T.J. and Webster, J.G.,1986, "Comparison Of Impedance Tomographic Reconstruction Algorithms", Clinical Physics and Physiological Measurement, vol.8 supp A, pp.55 - 62.

Yorkey, T., Webster, J. and Tompkins, W., 1987. "Comparing reconstruction algorithms for electrical impedance tomography", Transactions on Biomedical Engineering, vol.BME-34, No. 11, pp.843 - 852.

Watkins, D.S., 1991, Fundamental of Matrix Computation. New York : John Wiley & Sons.

Guardo, R., Boulay, C., Murray, B., and Bertrand, M., 1991. "An experimental study in electrical impedance tomography using backprojection reconstruction", IEEE Transactions on Biomedical Engineering, vol.3, No. 7, pp.617-627.

10. Responsibility notice

The authors are the only responsible for the printed material included in this paper